# Squeezed vacuum from a monolithic optical parametric oscillator

**G. Breitenbach, T. Müller, S. F. Pereira, J.-Ph. Poizat,\* S. Schiller, and J. Mlynek**

*Fakultät für Physik, Universität Konstanz, D-78434 Konstanz, Germany*

We have developed a stable, reliable source of continuous-wave squeezed vacuum at 1064 nm, using a subthreshold monolithic lithium niobate optical parametric oscillator. Quantum-noise reduction below the vacuum noise level in a bandwidth of 30 MHz with a maximum of $5.5 \pm 0.2$ dB at 2 MHz is demonstrated. The reconstruction of the Wigner function of a continuous-wave, strongly squeezed-vacuum state is obtained. © 1995 Optical Society of America

## 1. INTRODUCTION

Squeezed states of light have been successfully demonstrated in several different schemes, for both phase and amplitude quadratures of the electromagnetic field.[1] Among these schemes, the optical parametric oscillator (OPO) operating both below and above threshold has been verified to be a very good squeezing generator. In addition to the demonstration of a high degree of squeezing,[2-4] these devices have been used in several applications such as sub-shot-noise interferometry and spectroscopy, noise reduction in optical amplification, and back-action-evading measurements.[5-8] It has also been suggested that the solution of many challenging problems in quantum mechanics, such as quantum nondemolition measurements, noiseless amplification, and Schrödinger cats, can be pursued with OPO's.[9-11] For most of these experiments and proposals, OPO's with good stability and low loss are essential.

To realize a compact, stable, low-loss system for the generation of squeezed states of light, we employ a monolithic resonator. The monolithic resonator is a simple device that consists of a nonlinear crystal coated on both faces with reflecting dielectric coatings. Such a design ensures good mechanical stability and small losses. Furthermore, because of the short length of the cavity, the linewidth of such a resonator is broad compared with those at discrete cavities, which implies a broad bandwidth in the noise reduction. The performance of monolithic resonators has been successfully tested for second-harmonic generation and frequency downconversion and for the generation of nonclassical light such as twin beams and bright squeezing in second-harmonic generation.[12-14]

In this paper we combine these techniques to build a compact continuous-wave source of squeezed vacuum at 1064 nm. Our research is partially motivated by the possible application of such a squeezed-light source in planned gravitational wave interferometers and ultrasensitive polarimeters, which will operate at this wavelength.[15,16] In addition to the measurement of broadband squeezing, we applied the technique of optical homodyne tomography[17,18] to reconstruct, for the first time to our knowledge, the Wigner function of a strongly squeezed state in the continuous-wave regime.

The paper is organized as follows. In Section 2 we describe the experimental setup and characterize the OPO. In Section 3 we present the measurements of squeezing and the reconstruction of the Wigner function. Conclusions and future prospects are given in Section 4.

## 2. EXPERIMENTAL SETUP AND CHARACTERIZATION OF THE OPO

A general overview of the experimental setup is shown in Fig. 1. A frequency-doubled diode-pumped Nd:YAG laser (Lightwave Electronics Model 122) pumps a monolithic degenerate type-I OPO whose output is analyzed in a balanced homodyne detector.

The OPO is a 7.5-mm-long standing-wave resonator consisting of a LiNbO₃ crystal doped with 5% MgO. The end faces of the crystal are polished spherically, with 10-mm radii of curvature. One end of the crystal is coated with a high reflector at both 1064 and 532 nm; the other side is the output coupler with transmission $T = 2.1\%$ at 1064 nm and high transmission at 532 nm. With this configuration, the nonresonant pump double passes the resonator to enhance the nonlinear coupling, so that the threshold is reduced. The faces perpendicular to the crystal $c$ axis are coated with gold for electro-optic modulation. The resonator is embedded in an aluminum oven whose temperature is actively controlled to a few millikelvins. The measured finesse of the OPO is 265, which, considering the free spectral range of 9 GHz, gives a linewidth of $2\Gamma = 34$ MHz (FWHM).

Crucial for the suitability of a resonator for the generation of strong squeezing is its escape efficiency $\rho = T/(T + A)$, where $T$ is the transmission of the output coupler and $A$ is the total internal round-trip loss of the resonator. The value of $\rho$ is equal to the maximum achievable degree of squeezing. For a monolithic resonator, it is not easy to measure the propagation losses $A$ and the output coupler transmission $T$ separately. A
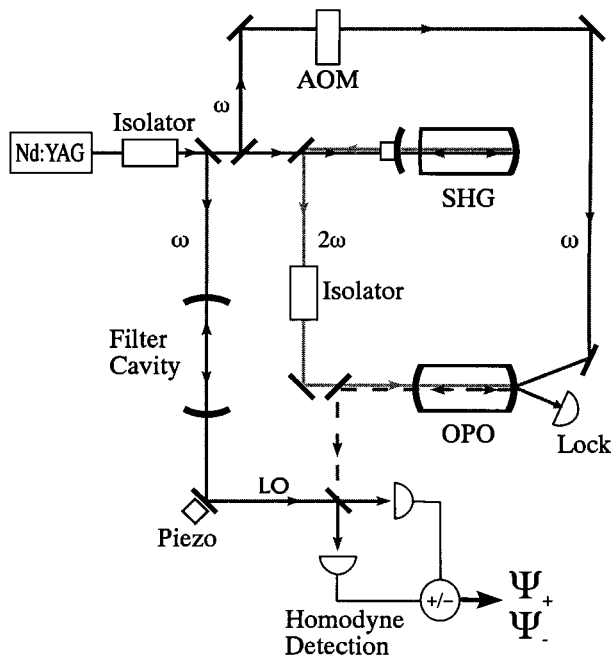
Fig. 1. Experimental scheme for the generation of squeezed vacuum with a monolithic LiNbO$_3$ resonator. AOM, acousto-optic modulator; SHG, second-harmonic generator; LO, local oscillator; piezo, piezoelectric mirror actuator.

direct way to determine the escape efficiency consists of measuring the conversion efficiencies for resonant second-harmonic generation or for parametric downconversion. For both processes the maximum conversion efficiency is equal to $\rho$. In previous experiments we measured maximum conversion efficiencies of 82% and 84% for frequency doubling and downconversion, respectively, at pump powers near 110 mW.[13,19] Correcting these values for the imperfect mode-matching results in an escape efficiency $\rho$ of 88%. Assuming perfect detection efficiency, the best degree of squeezing possible with this resonator is 9.5 dB.

A basic requirement for our system is temporal stability of the squeezing. This condition can be achieved by active stabilization, whereby the laser frequency is locked to the OPO cavity resonance and the frequency-doubling cavity is locked to the laser frequency. For the stabilization of the laser frequency a probe beam at 1064 nm is frequency shifted by 180 MHz with an acousto-optic modulator and is injected through the high-reflector end of the monolithic standing-wave cavity into a higher-order transverse mode, such that the laser frequency (the subharmonic of the OPO's pump frequency) coincides with the resonator's TEM$_{00}$ mode. Thus degenerate operation of the OPO is ensured. An error signal for the feedback to the laser is generated by a modified Pound–Drever technique,[20] in which the OPO crystal is modulated at 14.5 MHz, and the ensuing amplitude modulation of the probe wave is measured in reflection by a rf photodetector (see Fig. 1).

In fact, the high frequency stability of the laser and the OPO and the large OPO linewidth allow us to keep the laser frequency in resonance manually for several minutes. Most measurements shown here were therefore done without active stabilization of the laser.

The frequency-doubling cavity is independently locked

to the laser frequency with a similarly generated error signal controlling the cavity length by means of a piezoelectric mirror actuator.

The squeezed vacuum at the output of the OPO is combined with a strong local oscillator in a balanced homodyne detector.[21] As photodetectors we used passivated Epitaxx ETX500 InGaAs photodiodes with the covers removed. We measured the quantum efficiency to be 97%, using a Laser Instrumentation thermopile for calibration. The local oscillator is split off from the laser source and is filtered by a high-finesse cavity to reduce the excess amplitude noise of the diode-pumped Nd:YAG laser at frequencies of a few megahertz. The filter cavity is 50 cm long, with a bandwidth of 140 kHz. Figure 2 shows the spectral densities $\Psi_{\pm}$ of the photocurrents $i_{\pm}$ from the plus and the minus junctions of the homodyne detector for the beams before and after the filter cavity. A comparison of the traces shows that the excess noise of the laser is strongly suppressed by the filter cavity, so that the local oscillator is shot-noise limited at frequencies $\geq 1$ MHz. The suppression of a strong coherent modulation applied to the local oscillator is better than 20 dB. The shot-noise level, determined by comparison of $\Psi_{+}$ and $\Psi_{-}$ when the open port of the beam splitter has vacuum input, is accurate to 0.3 dB for a wide range of frequencies. When the balancing of power in the two detectors is optimized for a particular frequency, the accuracy is of the order of 0.2 dB. With a local oscillator power of 2 mW the shot-noise level is 14 dB above the electronic noise level of the detectors at lower frequencies and 5 dB for frequencies above 24 MHz.

The alignment as well as the mode matching of the pump into the OPO were optimized by operation of the OPO above threshold, as described in Ref. 19. Further optimization of the pump alignment and the OPO temperature was done by measurement of the parametric amplification of a small signal at 1064 nm injected into the high-reflector port of the cavity. With pump powers near the threshold power of 28 mW, parametric gain as high as 170 was observed.
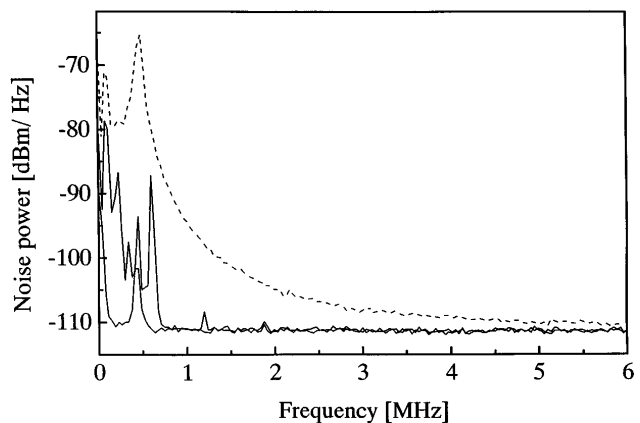


Fig. 2. Spectral density of the amplitude noise of the diode-pumped Nd:YAG laser as a function of frequency. Shown are $\Psi_{+}$ before the filter cavity (top, dashed trace) and $\Psi_{+}$ after the filter cavity (middle, solid trace). The bottom trace shows $\Psi_{-}$ for both cases. The peak at 500 kHz is due to the relaxation oscillation of the laser. The second peak at 600 kHz in the trace of $\Psi_{+}$ after the filter cavity is the frequency modulation used for locking the cavity. The resolution bandwidth was 10 kHz.

## 3. MEASUREMENTS OF SQUEEZING

### A. Squeezing Spectrum

The squeezed vacuum from the OPO is detected by a measurement of the photocurrent fluctuations $i_-$ from the balanced homodyne detector. The resulting current is sent to a spectrum analyzer, where the spectral density $\Psi_-$ is recorded. The maximum noise enhancement $S_+$ (antisqueezing) and reduction $S_-$ (squeezing) correspond to the fluctuations of the quadrature components $\hat{x} = (\hat{a} + \hat{a}^\dagger)$ and $\hat{p} = (\hat{a} - \hat{a}^\dagger)/i$ of the electric-field operator $\hat{E}$. For a pump power $P$ and an analysis frequency $\Omega$, the spectra are given by[2,22]

$$S_\pm(\Omega, P) = \pm \frac{4\sqrt{P/P_{\mathrm{th}}}}{(\Omega/\Gamma)^2 + (1 \mp \sqrt{P/P_{\mathrm{th}}})^2}, \qquad (1)$$

where $\Gamma = 17$ MHz is the cavity linewidth (HWHM) and $P_{\mathrm{th}} = 28$ mW is the threshold power of the OPO. The measured spectral densities of the photocurrents are related to the spectra by

$$\Psi_\pm(\Omega, P) = \Psi_0[1 + \xi\rho S_\pm(\Omega, P)], \qquad (2)$$

where $\Psi_0$ is the spectral density for a vacuum-state input, $\rho$ is the escape efficiency of the resonator, and $\xi$ is the detection efficiency; the last includes propagation losses after the OPO, homodyne efficiency, and detector quantum efficiency.

Because we used broadband detectors that were calibrated between 1 and 30 MHz, we were able to record the whole spectrum of squeezing and antisqueezing by keeping the phase of the local oscillator constant at either minimum or maximum noise level. After subtracting the electronic noise and normalizing the squeezing and the antisqueezing to the shot-noise level, we obtained the traces shown in Fig. 3. The observation of squeezing at still higher frequencies was limited only by the bandwidth of the photodetectors employed in our detection scheme. The theoretical spectra are in good agreement with the experimental data, as shown by the curves presented in Fig. 3, where we used the total efficiency $\delta\xi$ and $P/P_{\mathrm{th}}$ as fit parameters.

The measurement of squeezing at a fixed frequency $\Omega = 2$ MHz is shown in Fig. 4, where trace (i) is the squeezing as a function of the local oscillator phase, trace (ii) is the shot noise, and trace (iii) is the squeezing when the phase of the local oscillator is fixed manually at the minimum noise level. By averaging the noise of trace (iii), we determine the squeezing level to be $5.5 \pm 0.2$ dB below the vacuum noise level. For the measurement shown, the pump power was approximately 3/4 the threshold power. Further increasing the pump power led to a higher gain, but additional noise degraded the squeezing. We believe that this effect is due to pump fluctuations, inasmuch as the pump was not shot-noise limited at 2 MHz. From measurements at lower pump powers we find the total efficiency of detection $\xi = 92\%$, which agrees within 2% with the following measured individual efficiencies: 98.5% homodyne, 98% propagation after the OPO, and 97% detector quantum efficiency. Once we corrected for these values, the inferred squeezing amounted to 7.9 dB outside the resonator.

### B. Squeezing Ellipse and Wigner Function

The usual way to represent a squeezed state of the electromagnetic field in the phase space defined by its quadrature components $x$ and $p$ is a depiction of an uncertainty region with the shape of an ellipse. The principal axes of this ellipse correspond to the standard deviation of the fluctuations in the (possibly rotated) squeezed and the antisqueezed quadrature components. The ellipse represents a contour of the Wigner function $W(x, p)$ of that state.

The Wigner function is a quasi-probability distribution in phase space, differing from a classical distribution mainly by the fact that it may be negative and by the fact that it cannot be measured directly, inasmuch as it is a joint distribution of the eigenvalues of two noncommuting observables.[23] What is measurable, though, for any pair of rotated quadrature components $\hat{x}_\theta = \hat{x}\cos(\theta) + \hat{p}\sin(\theta)$, $\hat{p}_\theta = -\hat{x}\sin(\theta) + \hat{p}\cos(\theta)$, are the marginal distributions $P_\theta(x_\theta) = \int_{-\infty}^{\infty} W[x_\theta \cos(\theta) -$
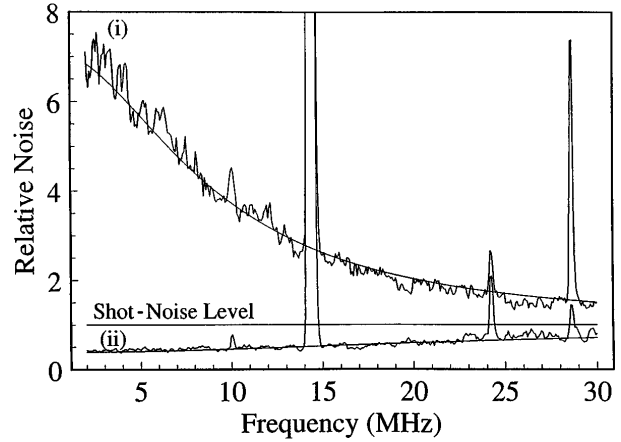


Fig. 3. Spectral density $\Psi_-$ as a function of the analysis frequency $\Omega$, with trace (i) being the antisqueezing spectrum and trace (ii) the squeezing spectrum. The theoretical expectations are denoted by the solid curves superimposed upon traces (i) and (ii). The peak at 14.5 MHz and its harmonic at 29 MHz come from the modulation of the doubling cavity used for locking. The resolution bandwidth was 100 kHz; the video bandwidth, 100 Hz.
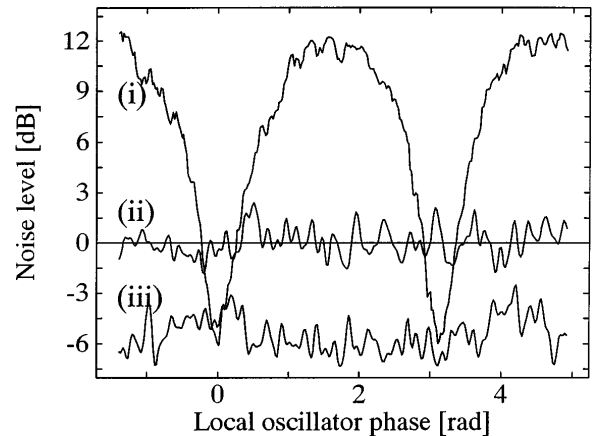


Fig. 4. Squeezed vacuum from the monolithic OPO. In trace (i) the phase of the local oscillator is being scanned; in trace (iii) the phase is fixed manually for minimum noise. One obtains the shot-noise level by averaging trace (ii). The resolution bandwidth was 100 kHz; the video bandwidth, 1 kHz.
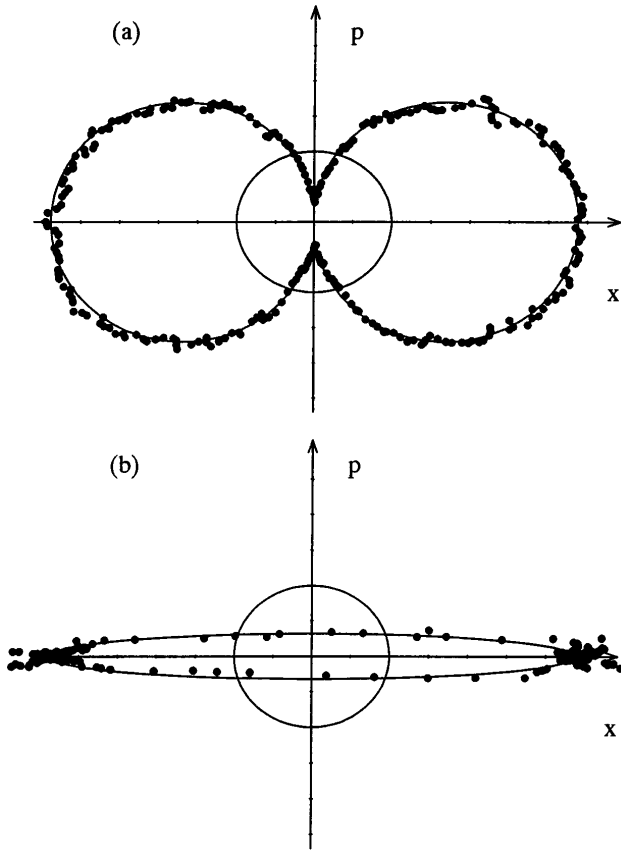
Fig. 5. (a) Standard deviations of the electric-field amplitudes of a squeezed-vacuum state in phase space. The circle represents the unsqueezed vacuum state. (b) The same data transformed into a squeezing ellipse. The points correspond to measured values corrected for total efficiency, and the curves represent the theoretical expectations.

$p_\theta \sin(\theta)$, $x_\theta \sin(\theta) + p_\theta \cos(\theta)] d p_\theta$.[17] These marginal distributions are classical probability distributions. For the case of a squeezed state, they are Gaussian. The recently established technique of optical homodyne tomography permits the reconstruction of the Wigner function from these marginal distributions by use of the inverse Radon transform.[17,18] Because the Wigner function is related to the density matrix through a Fourier transform, it is possible to determine completely the quantum-mechanical state of a system.

In the following discussion, we first show how to visualize the uncertainty region of the quantum-mechanical state of the light field in our experiment based on a measurement of the variances, and then we describe the reconstruction of its entire Wigner function.

The square roots of the experimental values of the variances (measured as in Fig. 4) correspond, when corrected for escape and detection efficiency and the electronic noise floor, to the standard deviation of the electric-field operator $\hat{E}$ in phase space as a function of the phase angle $\theta$. Its equation is given by $\Delta\hat{E}(\theta) = [(\Delta\hat{x})^2 \cos^2(\theta) + (\Delta\hat{p})^2 \sin^2(\theta)]^{1/2}$, which is the equation of a lemniscate. The phase-space representation of our experimental data is shown in Fig. 5(a). The circle represents the unsqueezed vacuum state. The principal axes of the lemniscate, $a = \Delta\hat{x}$ and $b = \Delta\hat{p}$, correspond to maximum noise suppression or enhancement in the respective quadrature component.

The variances of the $E$ field can be thought of as being projections of the uncertainty region in phase space onto the direction of observation determined by the phase angle $\theta$. Geometrically, this means that the $E$-field variances form the pedal curve of the uncertainty region.[24] Therefore the uncertainty region and thus the contour of the Wigner function are calculated with the transformation

$$[r(\theta)\cos(\theta),\ r(\theta)\sin(\theta)] \Rightarrow \left[ \frac{a^2}{r(\theta)}\ \cos(\theta),\ \frac{b^2}{r(\theta)}\ \sin(\theta) \right] \cdot$$
(3)

The result for a 4-dB squeezed-vacuum state is shown in Fig. 5(b). The area of the ellipse and the circle are approximately equal, as is expected for a minimum uncertainty state.

Although this transformation of the values of the variances to the contour of the Wigner function is correct for a minimum uncertainty state, it is not correct for arbitrary states of the light field. The information contained in the variances is in general not sufficient to infer the geometrical shape of the uncertainty region.

We gain more information about the state of the light field by recording not just the variance but rather the whole distribution $P_\theta(x_\theta)$ of the electric-field fluctuations.
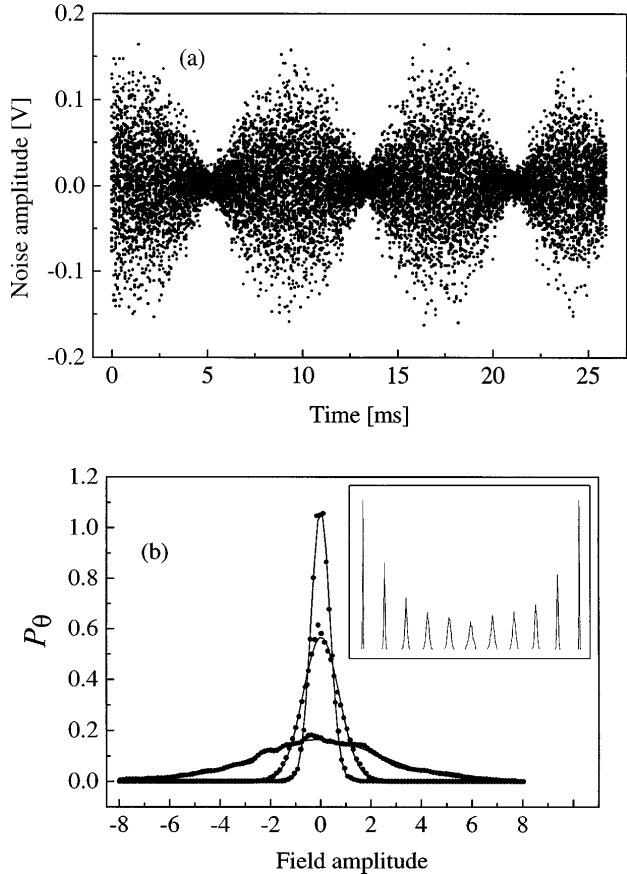




Fig. 6. (a) Noise of the photocurrent $i_-$ of the squeezed vacuum from the OPO at 2 MHz as a function of the local oscillator phase. The detection bandwidth is 100 kHz. (b) Distributions of the photocurrent fluctuations for maximum squeezing, shot noise, and maximum antisqueezing. The curves are fits of Gaussian distributions. The inset shows the distributions for eleven different phase angles from 0 to $\pi$.
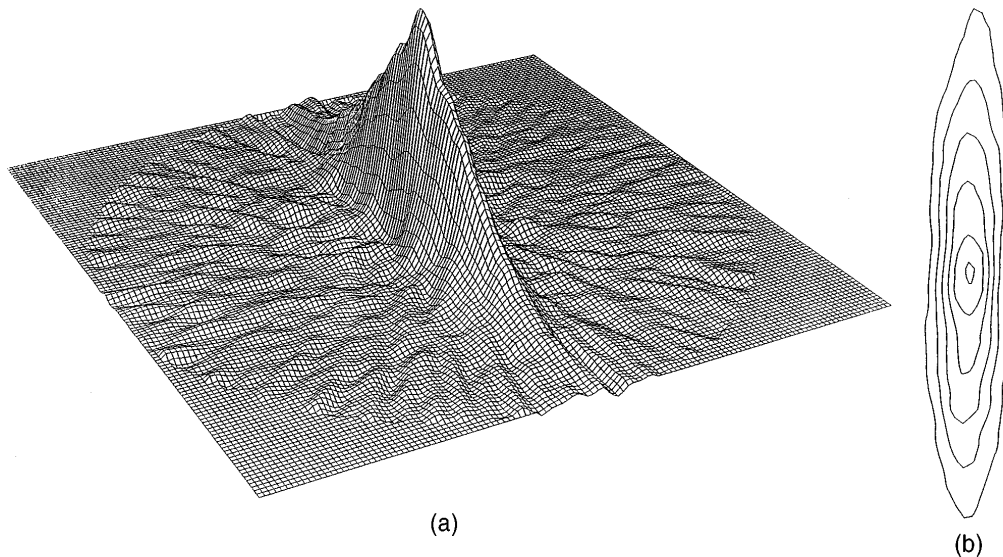
Fig. 7. (a) Reconstruction of the Wigner function for the squeezed vacuum. (b) Contour plot of the Wigner function. The ellipticity of the contours is slightly smaller than in Fig. 5 because no corrections for the detection efficiency were made.

As mentioned above, this procedure allows us to employ the method of optical homodyne tomography to determine the Wigner function completely. The inverse Radon transform corresponds in two dimensions to the step of backprojecting the variances, carried out above.

For a squeezed-vacuum mode of frequency $\Omega$ relative to the carrier optical frequency, the Wigner function is given by

$$W_{\text{sq}}(x, p) = (1/2\pi)\exp\left(-\frac{1}{2}\{[1 + \rho S_-(\Omega)]x^2 + [1 + \rho S_+(\Omega)]p^2\}\right), \qquad (4)$$

where $S_+$ and $S_-$ are defined by Eq. (1). Thus there is a spectrum of Wigner functions that differ in the ratio of their half-widths. For our reconstruction we chose the field mode at $\Omega = 2$ MHz.

Following the procedure described in Ref. 18, we first obtained the distributions of the electric-field amplitude at several different phase angles in phase space. The intermediate-frequency output of the spectrum analyzer at 2 MHz with a resolution bandwidth of 100 kHz, was recorded by a Nicolet 400 digitizing oscilloscope, as the local oscillator phase was slowly scanned. In this way it is possible to observe the variance of the electric field directly on the spectrum analyzer while accumulating the amplitude data. A typical trace of the resulting photocurrent fluctuations is shown in Fig. 6(a). We divided this time trace of 161,000 points into 79 sections corresponding to 79 different phase angles. For each phase angle interval the time-dependent amplitude noise was sorted into 128 bins. Thus histograms of 128 bins at 79 different phase angles $\theta$ were created, each having the shape of a Gaussian [Fig. 6(b)]. These histograms correspond, when normalized, to the Gaussian distributions of the amplitude noise at different phase angles.

Finally, the collection of histograms was transformed with the inverse Radon transform. The main part of the inversion algorithm consists of a convolution of the measured histogram values with a given filter function (filtered backprojection). A quadratic regularization was used to approximate this filter function. The Wigner function and its contour lines are shown in Fig. 7. Note that no corrections for detection and escape efficiency were made. For the chosen parameters, the numerical error of this reconstruction process is estimated to be less than 2%, which is consistent with a comparison of the ratio of the two half-widths of the Wigner-function sections at $x = 0$ and $p = 0$ and the directly observed squeezing and antisqueezing of 5.5 and 11 dB for this measurement.

## 4. CONCLUSIONS

In conclusion, we have used a monolithic continuous-wave OPO pumped below threshold to generate squeezed vacuum at 1064 nm. With this device 5.5 dB of squeezing was observed at a frequency of 2 MHz, and the whole squeezing spectrum from 2 to 30 MHz was recorded. Furthermore, the Wigner function of the squeezed-vacuum state was reconstructed. With the same device we have generated a beam of bright squeezed light by the process of parametric deamplification. 4-dB noise reduction in the amplitude noise of a 0.25-mW beam was achieved.[25] The level of detected squeezing was limited mainly by the finite detection efficiency and the noise of the pump laser. We plan a further investigation of the effect of the latter in the future.

The reconstruction of the Wigner function of a squeezed state represents a first step in a complete experimental characterization of a squeezed state. Because of the high degree of squeezing and its good stability, the experimental determination of the photon statistics and density-matrix elements in Fock-state representation appears to be possible.[26]

We believe that, beyond the demonstration of the performance of monolithic resonators as very stable, compact squeezing sources with a high degree of squeezing, they can be useful in several applications of squeezed light. The broad bandwidth makes it suitable for spectroscopic investigations, and its simplicity should make

proposed experiments that require more than one source of squeezed light more accessible.

*Permanent address, Institut d'Optique, B. P. 147, 91403 Orsay, France.

## REFERENCES

1. See J. Opt. Soc. Am. B **4** (1987); J. Mod. Opt. **34** (1987) (special issues on squeezed states of light); Appl. Phys. B **55,** (1992) (special issue on quantum-noise reduction in optical systems).
2. L.-A. Wu, H. J. Kimble, J. L. Hall, and H. Wu, "Generation of squeezed states by parametric down conversion," Phys. Rev. Lett. **57,** 691 (1986).
3. E. S. Polzik, J. Carri, and H. J. Kimble, "Atomic spectroscopy with squeezed light for sensitivity beyond the vacuum-state limit," Appl. Phys. B **55,** 279 (1992).
4. J. Mertz, T. Debuisschert, A. Heidmann, C. Fabre, and E. Giacobino, "Improvements in the observed intensity correlation of optical parametric oscillator twin beams," Opt. Lett. **16,** 1234 (1991).
5. M. Xiao, L.-A. Wu, and H. J. Kimble, "Precision measurement beyond the shot-noise limit," Phys. Rev. Lett. **59,** 278 (1987); P. Grangier, R. E. Slusher, B. Yurke, and A. La Porta, "Squeezed-light-enhanced polarization interferometer," Phys. Rev. Lett. **59,** 2153 (1987).
6. E. S. Polzik, J. Carri, and H. J. Kimble, "Spectroscopy with squeezed light," Phys. Rev. Lett. **68,** 3020 (1992).
7. Z. Y. Ou, S. F. Pereira, and H. J. Kimble, "Quantum noise reduction in optical amplification," Phys. Rev. Lett. **70,** 3229 (1993).
8. S. F. Pereira, Z. Y. Ou, and H. J. Kimble, "Back-action evading measurements for quantum nondemolition detection and quantum optical tapping," Phys. Rev. Lett. **72,** 214 (1994)
9. B. Yurke, "Optical back-action-evading amplifiers," J. Opt. Soc. Am. B **2,** 732 (1985); P. Smith, M. Collett, and D. F. Walls, "Quantum nondemolition measurement with an optical parametric amplifier," Opt. Commun. **102,** 1051 (1993).
10. I. E. Protsenko, L. A. Lugiato, and C. Fabre, "Spectral analysis of the degenerate optical parametric oscillator as a noiseless amplifier," Phys. Rev. A **50,** 1627 (1994).
11. L. Krippner, W. J. Munro, and M. D. Reid, "Transient macroscopic quantum superposition states in degenerate parametric oscillation: calculations in the large quantum limit using the positive *P*-representation," Phys. Rev. A **50,** 4330 (1994).
12. W. J. Kozlovsky, C. D. Nabors, and R. L. Byer, "Efficient second harmonic generation of a diode-laser-pumped Nd:YAG laser using monolithic MgO:LiNbO$_3$ external resonant cavities," IEEE J. Quantum Electron. **24,** 913 (1988); W. J. Kozlovsky, C. D. Nabors, R. C. Eckardt, and R. L. Byer, "Monolithic MgO:LiNbO$_3$ doubly resonant optical parametric oscillator pumped by a frequency-doubled diode-laser-pumped Nd:YAG laser," Opt. Lett. **14,** 66 (1989).
13. R. Paschotta, K. Fiedler, P. Kürz, R. Henking, S. Schiller, and J. Mlynek, "82% Efficient continuous-wave frequency doubling of 1.06 $\mu$m with a monolithic MgO:LiNbO$_3$ resonator," Opt. Lett. **19,** 1325 (1994).
14. C. D. Nabors and R. M. Shelby, "Two-color squeezing and sub-shot noise signal recovery in doubly resonant optical parametric amplifier," Phys. Rev. A **42,** 556 (1990); A. Sizmann, R. J. Horowicz, G. Wagner, and G. Leuchs, "Observation of amplitude squeezing of the up-converted mode in second harmonic generation," Opt. Commun. **80,** 138 (1990); P. Kürz, R. Paschotta, K. Fiedler, and J. Mlynek, "Bright squeezed light by second-harmonic generation in a monolithic resonator," Europhys. Lett. **24,** 449 (1993); R. Paschotta, M. Collett, P. Kürz, K. Fiedler, H.-A. Bachor, and J. Mlynek, "Bright squeezed light from a singly-resonant frequency doubler," Phys. Rev. Lett. **72,** 3807 (1994).
15. A. Giazotto, "Wide-band measurement of gravitational waves: the VIRGO project," Nuovo Cimento C **6,** 955 (1992); J. Hough, G. P. Newton, N. A. Robertson, H. Ward, B. F. Schutz, K. Danzmann, A. Rüdiger, R. Schilling, and W. Winkler, "Proposal for a 600 m laser interferometric gravitational wave antenna—GEO 600," Internal Rep. 190 (Max Planck Institut für Quantenoptik, Munich, 1994).
16. D. Bakalov, G. Cantatore, G. Carugno, S. Carusotto, P. Favaron, F. Della Valle, I. Gabrielli, U. Gastaldi, E. Iacopini, P. Micossi, E. Milotti, R. Onofrio, R. Pengo, F. Perrone, G. Petrucci, E. Polacco, C. Rizzo, G. Ruoso, E. Zavattini, and G. Zavattini, "PV-LAS: vacuum birefringence and production and detection of nearly massless, weakly coupled particles by optical techniques," Nucl. Phys. B Proc. Suppl. **35,** 180 (1994).
17. K. Vogel and H. Risken, "Determination of quasiprobability distributions in terms of probability distributions for the rotated quadrature phase," Phys. Rev. A **40,** 2847 (1989).
18. D. T. Smithey, M. Beck, M. G. Raymer, and A. Faridani, "Measurement of the Wigner distribution and the density matrix of a light mode using optical homodyne tomography: application to squeezed states and the vacuum," Phys. Rev. Lett. **70,** 1244 (1993).
19. G. Breitenbach, S. Schiller, and J. Mlynek, "81% Conversion efficiency in frequency-stable continuous-wave parametric oscillation," J. Opt. Soc. Am. B **12,** 2095 (1995).
20. R. Drever, J. Hall, F. Kowalski, J. Hough, G. Ford, A. Munley, and H. Ward, "Laser phase and frequency stabilization using an optical resonator," Appl. Phys. B **31,** 97 (1983).
21. H. P. Yuen and V. W. S. Chen, "Noise in homodyne and heterodyne detection," Opt. Lett. **18,** 177 (1983); B. Schumaker, "Noise in homodyne detection," Opt. Lett. **19,** 189 (1984).
22. M. J. Collett and D. F. Walls, "Squeezing spectra for nonlinear optical systems," Phys. Rev. A **32,** 2887 (1985).
23. E. P. Wigner, "On the quantum correction for thermodynamic equilibrium," Phys. Rev. **40,** 749 (1932).
24. R. Loudon, "Graphical representation of squeezed-state variances," Opt. Commun. **70,** 109 (1989).
25. S. Schiller, G. Breitenbach, S. F. Pereira, R. Paschotta, A. G. White, and J. Mlynek, "Generation of continuous-wave bright squeezed light," in *Laser Frequency Stabilization and Noise Reduction*, Y. Shevy, ed., Proc. Soc. Photo-Opt. Instrum. Eng. **2378,** 91 (1995).
26. U. Leonhardt, Department of Physics, Humboldt-Universität, 12484 Berlin, Germany (personal communication, 1995); M. G. Raymer, Department of Physics, University of Oregon, Eugene, Oregon 97403 (personal communication, 1995); G. M. D'Ariano, C. Macchiavello, and M. G. A. Paris, "Detection of the density matrix through optical homodyne tomography without filtered back projection," Phys. Rev. A **50,** 4298 (1994).